

S. Mokrane · L. Makhloufi · H. Hammache · B. Saidani

## Electropolymerization of polypyrrole, modified with germanium, on a passivated titanium electrode in aqueous nitrate solution: new results on catalytic reduction of protons and dissolved oxygen

Received: 20 August 1999 / Accepted: 6 July 2000 / Published online: 4 April 2001  
© Springer-Verlag 2001

**Abstract** Conductive polypyrrole (PPy) films and PPy films containing Ge microparticles were synthesized by anodic oxidation of pyrrole in acidic nitrate solutions using a bare passivated titanium electrode. Well-adhering black PPy films were obtained both under galvanostatic and potentiodynamic polarization. After the formation of the PPy film, during the first anodic cycle, an increase of the anodic deposition current with the number of cycles was observed, revealing the increase of conductivity of the growing film. The variations of the electrode surface area were estimated by impedance spectroscopy measurements. The kinetics of the PPy film formation is controlled by diffusion of the Py monomer in the solution. The diffusion coefficient, estimated by two different methods, was ca.  $2 \times 10^{-6} \text{ cm}^2 \text{ s}^{-1}$ . The reduction rate of oxygen and protons at the Ti/PPy/Ge electrodes depends on how the Ge microparticles are incorporated in the PPy film. Optimum conditions for this incorporation are realized with thin PPy films and high Ge loading. Thermogravimetric analysis shows that the PPy film containing Ge microparticles is more thermally stable than the blank PPy film.

**Keywords** Conducting polymers · Polypyrrole · Polymer-modified electrode · Cyclic voltammetry · Surface roughness

### Introduction

Incorporation of metal microparticles (Pt [1]) in a polypyrrole (PPy) film leads to chemical modification of the electrode surface, which results in control of the rate and selectivity of electrochemical reactions at the elec-

trode-electrolyte interface. These Pt particles [1] are distributed three-dimensionally in the PPy film in the porous polymer [2]. The resulting polymer-modified electrode shows electrocatalytic activity towards oxidation of hydrogen. Moreover, the reduction of oxygen in  $0.1 \text{ mol dm}^{-3} \text{ LiClO}_4$  in dimethyl sulfoxide (DMSO) has been studied [3] with the use of this electrode as a second model system in, for example, battery technology [4].

Electrocatalysis using electrodes coated with electroactive-modified polymers, electroactive composites and microheterogeneous systems has been extensively reviewed [5, 6, 7]. These electrodes have permitted the enhancement of the selectivity and sensitivity of many important electroanalytical reactions and the use of conducting polymer films in amperometric biosensors. Different compounds are used for modification of the PPy electrodes, e.g. nickel(II) complexes [8], Pt particles [1, 3], etc. Typically, electropolymerization of PPy was carried out in organic solvent solutions (e.g. acetonitrile containing tetraalkylammonium perchlorate or tetrafluoroborate as supporting electrolytes [9, 10]) with noble metal electrodes, such as Pt or Au, as working electrodes.

In the present work, we describe results on the kinetics of electrochemical polymerization of Py in aqueous acidic nitrate solution on a passivated bare titanium electrode (without PPy film on the titanium electrode as the initial conditions). To our knowledge, no systematic study of the kinetics of electrodeposition of a PPy film on such a bare electrode has been published until now. The first results on the preparation of a Ge-PPy film-coated Ti electrode and the reduction of protons and dissolved oxygen at this modified electrode are also presented.

### Experimental

Electropolymerization of PPy, chronoamperometry and chronopotentiometry were carried out using a Tacussel PGP 201 potentiostat/galvanostat coupled to a Hewlett Packard 250 personal computer under "voltmaster" software (Radiometer, Copenhagen). The impedance spectroscopy measurements, used for estimation of the

S. Mokrane · L. Makhloufi (✉) · H. Hammache · B. Saidani  
Laboratoire d'Electrochimie et Corrosion,  
Institut de Chimie Industrielle, Université de Béjaia,  
06000 Béjaia, Algeria  
E-mail: l.makhloufi@netcourrier.com  
Fax: +213 34 21 43 32

PPy film surface area, were performed using a frequency response analyzer (Tacussel, type ZCPI30T) monitored by a microcomputer. Thermogravimetric analysis of the PPy and Ge-PPy films was carried out between 25 and 750 °C with a heating rate of 10 °C min<sup>-1</sup> under an argon atmosphere. The thermogravimetrograms were recorded using a Setaram TG-DTA92 model thermal analyzer equipped with a 92-16.18 Setaram furnace and a CS 92 Setaram interface. The PPy films were investigated by scanning electron microscopy (SEM) coupled with energy dispersive X-ray (EDX) analysis (type Leika 440). The electrochemical experiments were made in a conventional three-electrode one-compartment cell, under argon at 25 °C. The working electrode was made of a titanium disk (area 1 cm<sup>2</sup>) polished with a 1200-grade emery paper and washed with bi-distilled water before each experiment. A platinum gauze was used as the auxiliary electrode and all potentials were measured versus the saturated calomel electrode (SCE), separated from the bulk electrolyte by a compartment containing the supporting electrolyte.

The PPy films were electrochemically grown on a passivated titanium electrode under cyclic voltammetry conditions at a potential scan rate of 10 mV s<sup>-1</sup> between -0.12 and 1.5 V, or under potentiostatic control at 0.8 V in 0.1 mol dm<sup>-3</sup> KNO<sub>3</sub> and HNO<sub>3</sub> containing Py at different concentrations between 0.0058 and 0.8 mol dm<sup>-3</sup>. The aqueous nitrate solution is the only one out of over 20 electrolytes containing low molecular weight anions which is successfully used for coating less noble metals [11]. A 10<sup>-4</sup> mol dm<sup>-3</sup> solution of germanium ions, used for modification of the PPy films, was prepared from germanium metallic powder attacked by hot sulfuric acid [12]. The modification was carried out at -0.7 V under potentiostatic control. The reduction of protons on the Ge-PPy film electrodes was conducted in an acidic solution of KNO<sub>3</sub> and HNO<sub>3</sub> (pH 2). Reduction of oxygen was performed in a DMSO solution of LiClO<sub>4</sub> in the absence of water, as previously described [3].

All electrolytes used were prepared using Prolabo p.a. quality products and bi-distilled water. All experiments were carried at ambient temperature (24 ± 1 °C).

## Results and discussion

### Voltammetric studies

The PPy films were prepared by oxidation of the Py monomer on a passivated titanium electrode. A typical cyclic voltammogram for this electrode in 0.1 mol dm<sup>-3</sup> KNO<sub>3</sub> and HNO<sub>3</sub>, pH 2 (called the base solution), with a linear potential sweep (10 mV s<sup>-1</sup>) between the open circuit potential and 1.5 V, is shown in Fig. 1. The polarization curve, in the absence of pyrrole in the solution, shows no oxidation current over a large potential range (-0.2 to +1.3 V). Beyond this range, oxygen evolution takes place, as can be seen in this figure. Note that the thermodynamic potential of oxygen evolution in this solution (1.23-0.06 pH) is about 0.87 V vs. SCE.

When 0.1 mol dm<sup>-3</sup> pyrrole is present in the base solution, the cyclic voltammogram (Fig. 1, curve 2) shows an irreversible anodic peak attributed to the electro-oxidation of pyrrole. The use of Py as received and Py freshly distilled under nitrogen leads to similar polarization curves. Only one forward scan suffices in order to obtain a black uniform film on the titanium electrode.

Oxidation of the PPy film-coated titanium electrode in a Py-free electrolyte solution was studied to determine

the contribution of the oxygen discharge at the PPy electrode during the electropolymerization of PPy (Fig. 2). We can see that the anodic current density resulting from the evolution of oxygen at the Ti/PPy electrode is negligible for potential lower than 1.3 V. This fact precludes the possibility of a competitive discharge of the electrolyte during the electropolymerization on the PPy film-coated Ti electrode. Thus all the current recorded in the polarization curves during the PPy electropolymerization is only the result of the oxidation of the Py monomer. The overall voltammetric behaviour for monomer oxidation is in good agreement with those reported in the literature [13, 14].

Note that the surface area used in the literature [15] for calculation of the anodic current densities in the presentation of the polarization curves did not take into account surface roughness, which is an inherent characteristic of all polymer films formed using electrochemical techniques.

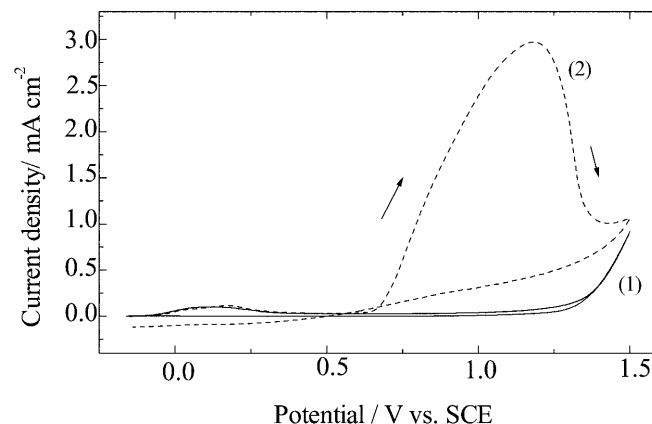


Fig. 1 Cyclic voltammograms of a titanium electrode in 0.1 mol dm<sup>-3</sup> (KNO<sub>3</sub> and HNO<sub>3</sub>), pH 2 (base solution), potential sweep rate 0.01 V s<sup>-1</sup>: (1) blank curve without pyrrole (Py); (2) with Py (C<sub>Py</sub> = 0.05 mol dm<sup>-3</sup>)

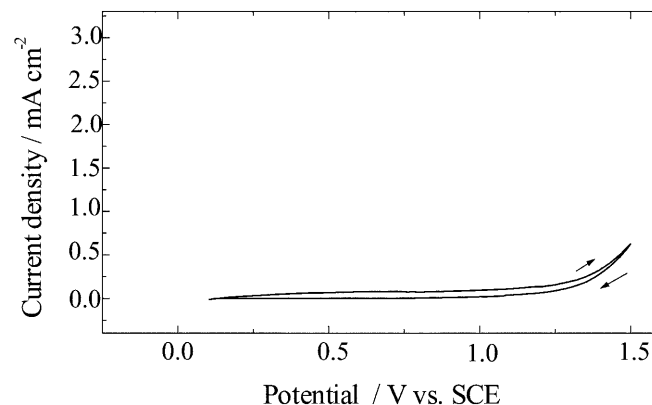


Fig. 2 Cyclic voltammogram of a PPy-coated titanium electrode in the base solution, potential sweep rate 0.01 V s<sup>-1</sup>, showing a negligible rate of oxidation and reduction of the electrolyte at this electrode

### Determination of the surface area of the PPy film-coated Ti electrodes

Once the titanium electrode is covered with a PPy film, the electropolymerization takes place on a PPy electrode. Then, the kinetics of the reaction could be influenced by the change of roughness of the deposit itself. Cheung et al. [16] reported highly connected microfibrils in the texture of the PPy film deposited on titanium. In order to estimate the “effective” electrode surface area resulting from the PPy deposition during the electropolymerization, and to exploit this electrode surface area in the calculation of the anodic current densities, we used electrochemical impedance spectroscopy [17, 18]. Figure 3 shows the impedance spectroscopy data plotted in the complex plane for a bare titanium electrode at the rest potential, in the Py-free electrolyte. The diagram exhibits a capacitive loop, close to a semi-circle between 100 kHz and 0.3 Hz, corresponding to the double layer capacitance,  $C_d$ , in parallel with the charge transfer resistance,  $R_t$ :

$$C_d = 1/(2\pi f_m R_t) \quad (1)$$

where  $f_m$  is the frequency at the apex of the capacitive loop. The nature of the charge transfer is unknown and it is outside the scope of the present work. The value of  $C_{d,0}$  ( $C_{d,0}$  corresponds to the Py-free electrolyte at a bare titanium electrode) is estimated to be  $11.1 \mu\text{F cm}^{-2}$ . Similar plots were obtained for the Ti/PPy electrode in the base solution. The PPy film was deposited by executing one anodic potential scan (without a reverse scan after the oxidation of the monomer), for different Py initial concentrations, between the rest potential and 1.500 V vs. SCE (Fig. 4). In this case the apex frequency,  $f_m$ , appears to be slightly higher than that obtained for a bare titanium electrode. Deposition of a PPy film causes a decrease in the charge transfer resistance,  $R_t$ , as shown in Figs. 3 and 4. This result is in agreement with those obtained by voltammetry, which have shown an increase of the peak current density with the increase of the initial Py concentration ( $C_{\text{Py}}$ ), i.e., an increase of the conductive nature of the PPy deposit with an increase of  $C_{\text{Py}}$ .

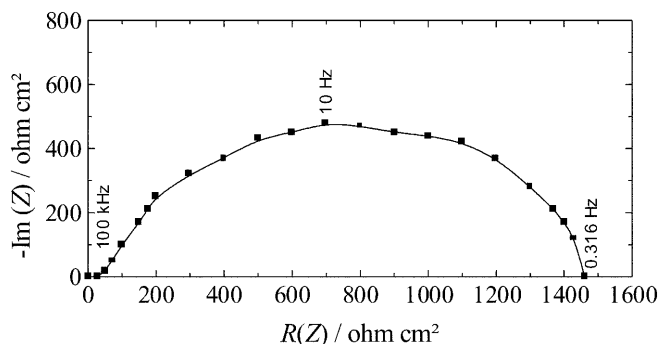


**Fig. 3** Complex plane impedance plot obtained at the rest potential for the bare titanium electrode in the base solution (Py-free electrolyte)

The values of the capacitances  $C_d$ , calculated from the data displayed in Fig. 4, are given in Table 1, where  $C_{d,0}$  corresponds to the Py-free electrolyte measured at a bare titanium electrode. Clearly, the  $C_d/C_{d,0}$  ratio, which characterizes the electrode roughness as referred to the surface of a bare titanium electrode at the rest potential, increases with the increase of the Py initial concentration. Thus, we have taken into account the roughness in the presentation of the anodic current density values in the kinetics curves presented in this work.

Figure 5a shows the evolution of the cyclic voltammograms of pyrrole electro-oxidation during repeated potential cycling for  $0.05 \text{ mol dm}^{-3}$  pyrrole in the base solution. This figure shows that the electropolymerization current decreases after the first cycle, which indicates partial inactivation of the Ti/PPy electrode by a relatively electro-inactive film. A similar result was found for polyaniline electrodeposition on Pt in malonic acid [19]. If we characterize this inhibition phenomenon by the ratio  $i_{\text{Pn}}/i_{\text{P1}} = f$  ( $i_{\text{P1}}$  corresponds to the peak current value obtained during the first anodic sweep and  $i_{\text{Pn}}$

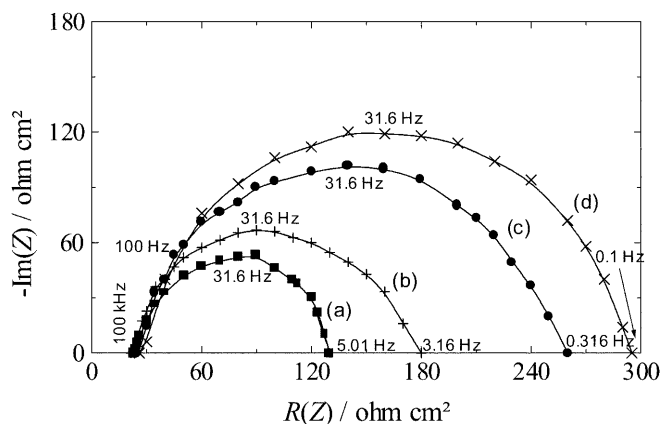


**Fig. 4** Complex plane impedance plot for various PPy coatings obtained by an anodic potential scan (from open circuit potential to 1.5 V at  $10 \text{ mV s}^{-1}$ ) in the different initial Py concentrations: (a)  $C_{\text{Py}} = 0.05 \text{ mol dm}^{-3}$ ; (b)  $C_{\text{Py}} = 0.03 \text{ mol dm}^{-3}$ ; (c)  $C_{\text{Py}} = 0.01 \text{ mol dm}^{-3}$ ; (d)  $C_{\text{Py}} = 0.0058 \text{ mol dm}^{-3}$  in the same reference base solution

**Table 1** Double layer capacitance  $C_d$  measured in the base solution of  $0.1 \text{ mol dm}^{-3}$  ( $\text{KNO}_3$  and  $\text{HNO}_3$ ), pH 2, for a titanium electrode coated with a PPy film. The latter is obtained by one oxidation scan between the rest potential and 1.500 V vs. SCE (without the reverse cathodic scan) for different Py initial concentrations.  $C_{d,0}$  corresponds to the double layer capacitance of the passivated titanium electrode without a PPy film

Initial concentration of Py ( $\text{mol dm}^{-3}$ ) used to obtain the PPy film	$C_d$ ( $\mu\text{F cm}^{-2}$ )	$C_d/C_{d,0}$
0	11.1	1
0.0058	18.5	1.7
0.01	21.3	1.9
0.03	31.9	2.9
0.05	46.2	4.2

corresponds to the peak current value corresponding to the subsequent sweeps  $n=2, 3, \dots, 10$ ), it is clear that during the second anodic sweep the peak current decreases by about 55% as compared to the value measured in the first sweep (Fig. 5b). From the third to the tenth cycle, this ratio increases slightly. This is probably due to the autocatalytic phenomenon of the successive PPy layers. The origin of this effect may be also related to an increase in the area of the reacting surface of the PPy film. Visual examination of the coating on the titanium electrode shows a black and adherent film.

The effect of the initial Py concentration on the PPy electropolymerization on the titanium electrode is illustrated in Fig. 6a and b. Certain inferences can be formulated based on the results depicted in this figure:

1. When the initial monomer concentration is lower than or equal to  $0.05 \text{ mol dm}^{-3}$  (Fig. 6a), the anodic peak current increases with the increase of the initial monomer concentration.

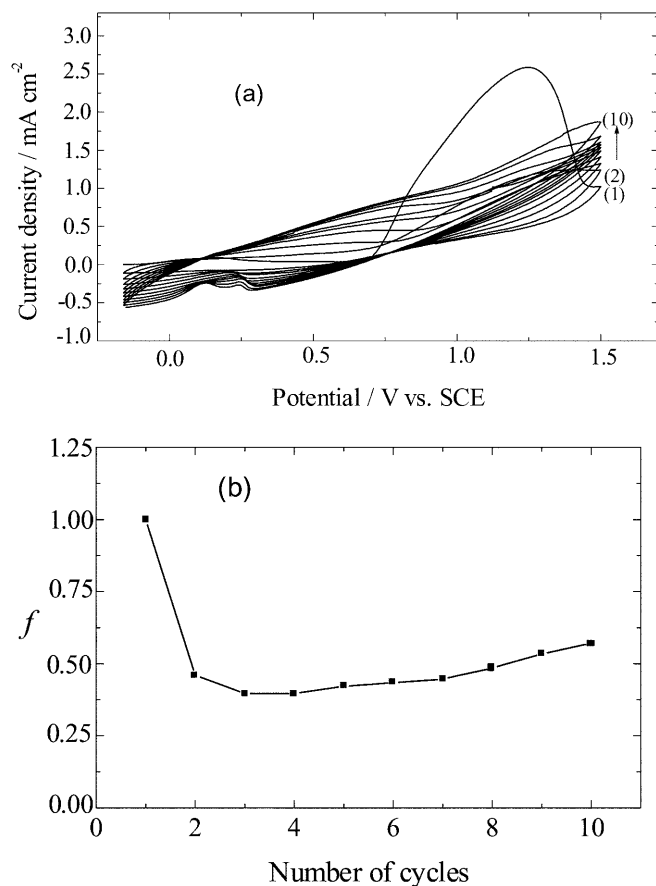


**Fig. 5** a Consecutive cyclic voltammograms of PPy electropolymerization on the titanium electrode, obtained in the base solution, in the presence of Py ( $C_{\text{Py}} = 0.05 \text{ mol dm}^{-3}$ ); potential sweep rate  $0.01 \text{ V s}^{-1}$ . b Curve, derived from a, which gives the ratio  $f = i_{p_n} / i_{p_1}$  versus the number of cycles;  $i_{p_1}$  is the anodic peak current for the first sweep and  $i_{p_n}$  for the  $n$ th sweep

2. The potentials of the oxidation peaks are shifted positively when the initial monomer concentration increases. This oxidation peak vanishes when the initial concentration of the monomer is larger than

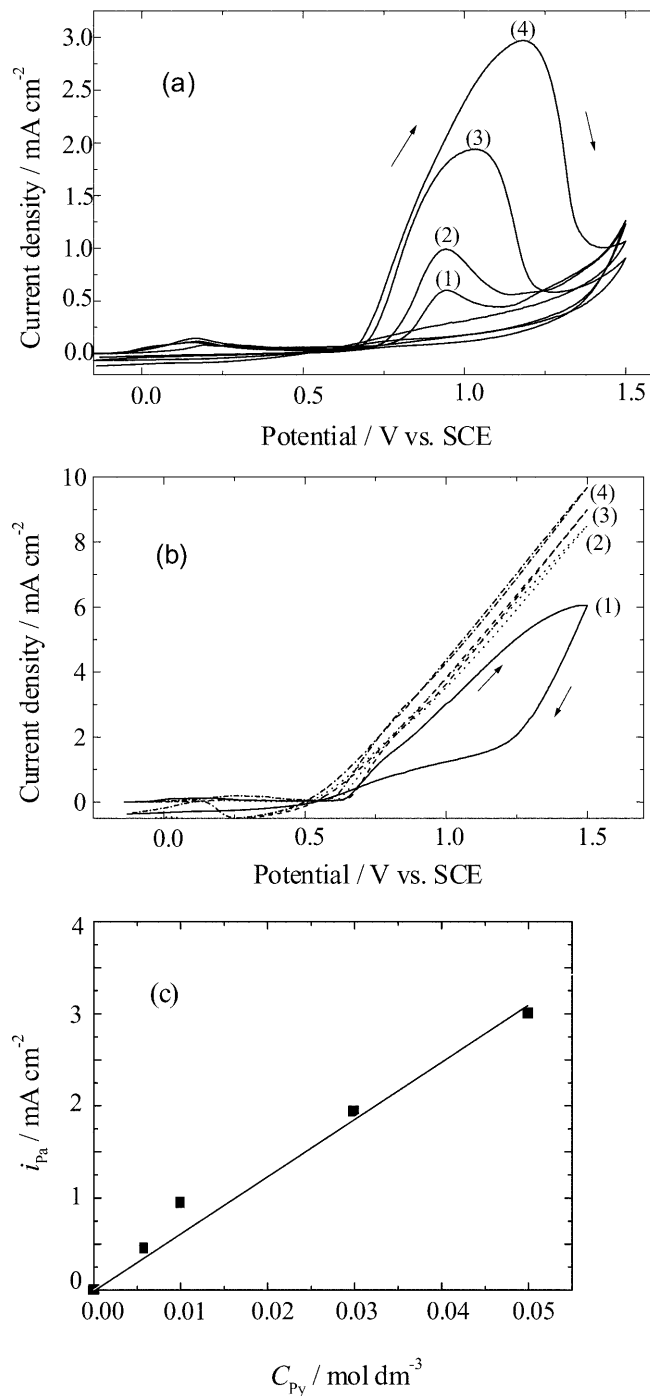


**Fig. 6** Cyclic voltammograms at a titanium electrode versus different Py initial concentrations in the base solution, potential sweep rate  $0.01 \text{ V s}^{-1}$ , for a (1)  $0.0058$ , (2)  $0.01$ , (3)  $0.03$ , (4)  $0.05 \text{ mol dm}^{-3}$ ; b (1)  $0.1$ , (2)  $0.2$ , (3)  $0.5$ , (4)  $0.8 \text{ mol dm}^{-3}$ . c Plot of anodic peak current density ( $i_{p_a}$ ) vs. initial Py concentration (curve derived from Fig. 6a above)

0.05 mol dm<sup>-3</sup> (Fig. 6b). The potential shifts result, presumably, from the ohmic potential drop due to the insulating nature of the polymer film.

Figure 6c shows the variation of the anodic peak current ( $i_{pa}$ ) versus the initial Py concentration in the range 0.0058–0.05 mol dm<sup>-3</sup>. This plot, being linear, implies that the rate of polymer formation is of first order with respect to the Py concentration. When the sweep rate ( $v$ ) is varied between 3 and 250 mV s<sup>-1</sup>, the anodic peak current increases with the increase of  $v$ , and the corresponding variation of  $i_{pa}$  is directly proportional to the square root of the sweep rate  $v^{1/2}$  (Fig. 7). This linear relationship between  $i_{pa}$  and  $v^{1/2}$  is consistent with a diffusion-controlled model of electroreduction, in agreement with the results of the literature in the case of PPy electropolymerization in alcoholic solution [20]. The oxidation peaks shifted to more positive potentials at scan rates larger than 7 mV s<sup>-1</sup> suggest that:

1. the electron transfer from the electrode to the PPy film is, presumably, slow;
2. the rate of electron transfer is controlled by diffusion of counterions at scan rates larger than 7 mV s<sup>-1</sup>; and/or
3. the ohmic potential drop across the film is significant.

From the dependence of the anodic peak current densities on the potential scan rate, we estimated the apparent diffusion coefficient of the monomer in the bulk solution,  $D$ , according to the following equation, for an irreversible system [21]:

$$i_p = 3.01 \times 10^5 n(\alpha n')^{1/2} D^{1/2} C v^{1/2} \quad (2)$$

where  $i_p$  is the anodic peak current density (A cm<sup>-2</sup>),  $n$  is the number of electrons transferred,  $n'$  is the number of electrons related to the rate-determining step ( $n=2$ ;

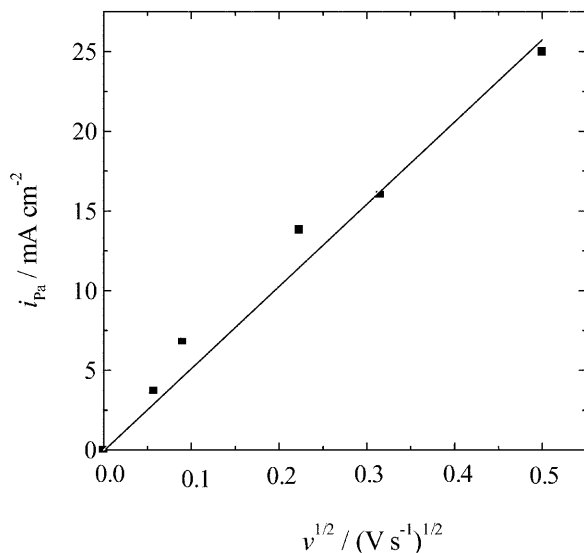


**Fig. 7** Plot of anodic peak current density vs. square root of the potential sweep rate ( $v^{1/2}$ ) for 0.05 mol dm<sup>-3</sup> Py in the base solution

$n'=1$ ;  $\alpha=0.5$  [22]),  $C$  (mol cm<sup>-3</sup>) is the initial monomer concentration and  $v$  is the potential scan rate (V s<sup>-1</sup>). Importantly, the value of the surface area used in the calculations takes account of the surface roughness. The slope of this straight line gives the diffusion coefficient,  $D=5.5 \times 10^{-6}$  cm<sup>2</sup> s<sup>-1</sup>.

A similar value ( $D=2.5 \times 10^{-6}$  cm<sup>2</sup> s<sup>-1</sup>) is determined using data from Fig. 6c. In the literature [23], the estimated apparent diffusion coefficient is found to be  $1 \times 10^{-10}$  cm<sup>2</sup> s<sup>-1</sup> if the same procedure as above is conducted with an initial presence of the polymer film on the substrate surface. This markedly low value of  $D$  corresponds to diffusion of the monomer in the PPy film when it is initially present on the substrate.

### Chronopotentiometry

In accord with the procedure used in industrial practice, the film-forming electropolymerization of pyrrole was performed at a constant current density. Figure 8a shows three typical potential-time curves for the PPy electropolymerization at the titanium electrode for three selected

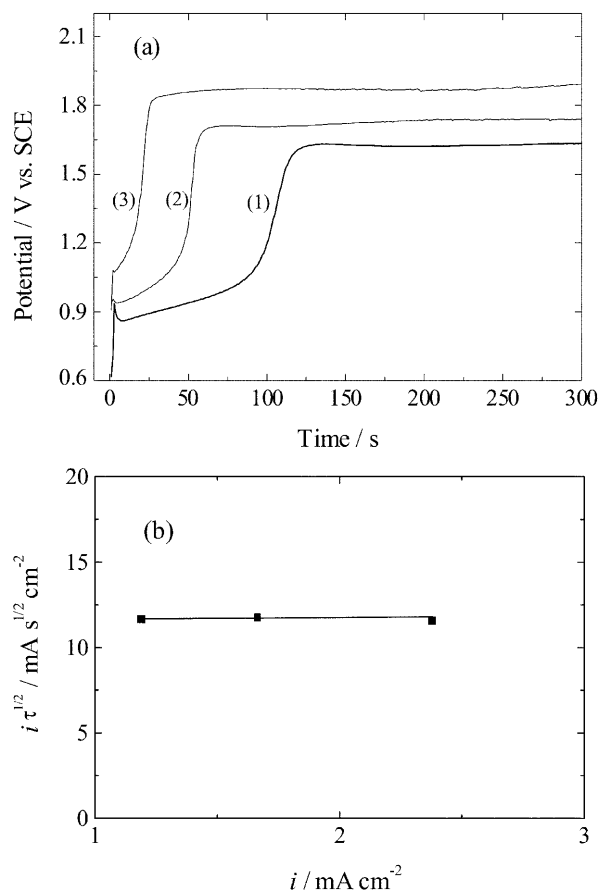


**Fig. 8** **a** Potential-time curves for the PPy electrodeposition on titanium for 0.05 mol dm<sup>-3</sup> Py in the base solution: (1)  $i=1.19$  mA cm<sup>-2</sup>, (2)  $i=1.67$  mA cm<sup>-2</sup>, (3)  $i=2.38$  mA cm<sup>-2</sup>. **b** Sand's plot,  $i\tau^{1/2}$  vs.  $i$ , for PPy electrodeposition on titanium (results derived from Fig. 8a)

current densities. The variation of the current density,  $i$ , has mainly two effects on the potential-time curves. The first is the decrease of the transition time ( $\tau$ ) with the increase of  $i$ . This means that, for the transition time which elapses after application of a constant current density, the concentration of the monomer becomes zero. It is found that the theoretically required relationship, the Sand's equation  $2i\tau^{1/2} = \pi^{1/2}nFC^{\circ}D^{1/2}$ , is obeyed (Fig. 8b). This result confirms that diffusion of Py in solution is the rate-determining step. In this case also the diffusion coefficient of Py in solution is  $D = 2 \times 10^{-6} \text{ cm}^2 \text{ s}^{-1}$ ; this value is in reasonable agreement with that found by voltammetry (see previous section). The second effect is a positive shift of the plateau potential, after  $\tau$  is reached, with the increase of the current density.

### Chronoamperometry

It has been reported that current transients recorded during the potentiostatic formation and growth of PPy films on electrodes from aqueous solutions are poorly reproducible [24]. This is particularly true when heterogeneous nucleation is taking place [25, 26]. Reproducible behaviour is observed only if the electrode surface state remains uniform and also if the solution

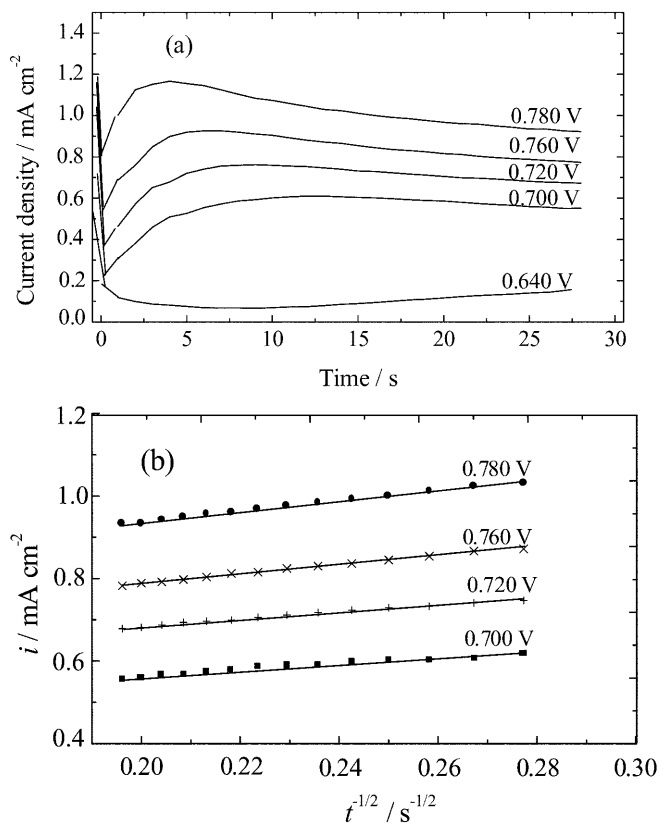


**Fig. 9** **a** Current transients for PPy electropolymerization on a passivated titanium electrode at different potentials (indicated at each curve) for  $0.05 \text{ mol dm}^{-3}$  Py in the base solution. **b** Chronoamperometric current-time curves ( $i$  vs.  $t^{-1/2}$ ) derived from data presented in Fig. 9a

composition does not change from one experiment to the other. Figure 9a shows current transients obtained during oxidation of  $0.05 \text{ mol dm}^{-3}$  pyrrole in a  $0.1 \text{ mol dm}^{-3}$  mixture of  $\text{KNO}_3$  and  $\text{HNO}_3$ , pH 2, at different potentials.

After a characteristic decay of current at short times (for the applied potential exceeding  $0.640 \text{ V vs. SCE}$ ) due to charging of the double layer, which may be accompanied by adsorption of pyrrole at the interface, as well as its oxidation to form oligomeric soluble species, it is followed by an increase of the current at intermediate times, due to the formation and growth of PPy centers on the electrode surface, and finally by decaying of the current at relatively long times, due to a process that limits the film growth rate. It can be seen that the intermediate time is shorter at the more positive applied potential. These applied potentials are chosen to be lower than the peak potential determined from the CV curve presented in Fig. 1. When the applied potential of a chronoamperometric experiment is close to the CV peak potential, the current quickly rises to reach a peak; then, over a time of seconds, only a current decay is observed.

The current decay over a long time was analyzed by plotting the current density as a function of  $t^{-1/2}$  (Fig. 9b). The linear dependence obtained confirms that the rate of diffusion controls the rate of the anodic reaction [22].

### Reduction of protons and oxygen at a modified PPy electrode containing Ge microparticles

Firstly, we present the way to obtain the incorporation of germanium particles into a PPy film; then we describe the reduction of protons and of oxygen on the PPy electrode containing the Ge microparticles.

#### Insertion of Ge microparticles

A titanium electrode potential was maintained at  $0.800 \text{ V vs. SCE}$  for 2–10 min in an unstirred solution containing  $0.1 \text{ mol dm}^{-3} \text{ KNO}_3$  and  $0.05 \text{ mol dm}^{-3}$  pyrrole. In effect, a black adherent film of PPy was formed. The electrode was weighed before and after the deposition of PPy. Then, the electrode was rinsed with water and placed in  $0.1 \text{ mol dm}^{-3} \text{ KNO}_3$  and the electrode potential was switched to  $-0.500 \text{ V vs. SCE}$  for 10 min in order to reduce the film and expel the anions. Next, the electrode was transferred to a solution containing germanium ions and the electrode potential was held at  $-0.700 \text{ V vs. SCE}$  in order to reduce and to incorporate the germanium into the PPy film.

#### Reduction of protons and oxygen at the Ge-containing PPy film

In order to characterize the modified electrode prepared above, cyclic voltammetry was conducted for the

reduction of protons in acidic nitrate solution and the reduction of oxygen in a solution of DMSO, which was 0.1 M in  $\text{LiClO}_4$ . This last solution was chosen in order to produce and regenerate oxygen, as reported in the literature [3, 27].

Cyclic voltammograms for reduction of oxygen at the PPy films containing Ge microparticles show a current plateau value, indicating the existence of a limiting current density. Figure 10 shows the limiting current as a function of the PPy film thickness for a given amount of germanium inserted. It can be seen that oxygen is reduced most efficiently at the thinnest films. These films contain the highest density of surface germanium sites. Since PPy is reduced, this film is not conducting [3, 28]. It has been suggested [29] that the permeability decreases as the electropolymerized films become thicker. Figure 11 shows that the limiting oxygen reduction current increases as the germanium content increases for a given constant thickness of a PPy film. The effect of varying the germanium deposition time is as great as that of the PPy. We can see in these two experiments

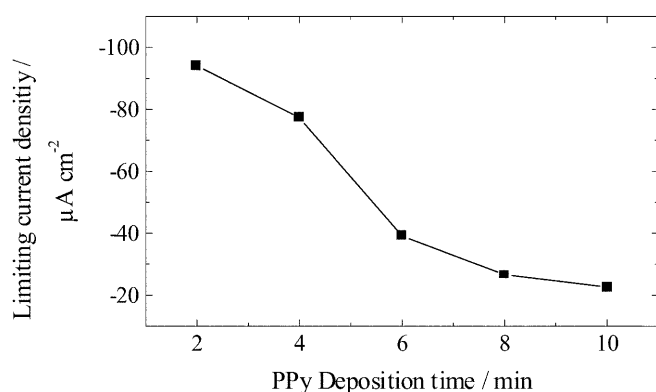


**Fig. 10** Variation of the limiting current density for oxygen reduction vs. the PPy deposition time (at 0.800 V vs. SCE) for  $0.1 \text{ mol dm}^{-3} \text{ LiClO}_4$  in DMSO; the content of germanium in the film (deposited for 20 min at  $-0.700 \text{ V vs. SCE}$ ) was constant

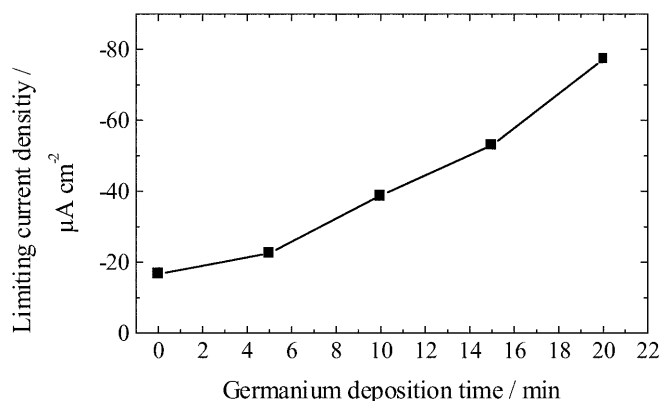


**Fig. 11** Variation of the limiting current density of oxygen reduction vs. germanium deposition time (at  $-0.700 \text{ V vs. SCE}$ ) for  $0.1 \text{ mol dm}^{-3} \text{ LiClO}_4$  in DMSO; the amount of PPy (deposited for 4 min at  $0.800 \text{ V vs. SCE}$ ) was constant

that the catalytic effect for the reduction of oxygen is more pronounced for a titanium electrode coated with a thin PPy film and a large amount of inserted germanium particles. Figure 12 shows similar behaviour concerning proton reduction at the Ge-containing PPy film-coated Ti electrode in an acidic nitrate solution. The result obtained provides more evidence of the catalytic effect of germanium inserted in the PPy film.

### Thermogravimetric analysis

Thermogravimetric measurements between 25 and  $750 \text{ }^\circ\text{C}$  of the PPy films and the PPy films containing Ge microparticles are given in Fig. 13. The mass loss appeared at about  $180 \text{ }^\circ\text{C}$  for the unmodified PPy film (curve 1 in Fig. 13) and showed a continuous decrease to reach, at  $750 \text{ }^\circ\text{C}$ , a weight loss of about 55% of the initial value. For the modified PPy, two distinct regions of the mass loss were observed (curve 2 in Fig. 13). The first mass loss appeared at  $145 \text{ }^\circ\text{C}$  and the second one at

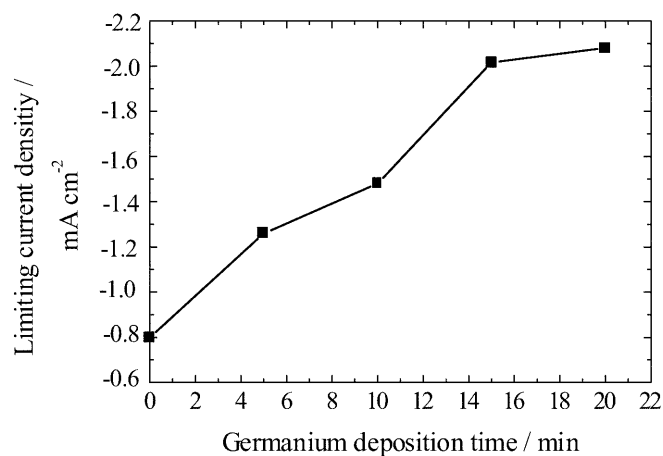


**Fig. 12** Variation of the limiting current of proton reduction vs. germanium deposition time (at  $-0.700 \text{ V vs. SCE}$ ) with a constant amount of PPy (deposited for 4 min at  $0.800 \text{ V vs. SCE}$ ) in the base solution

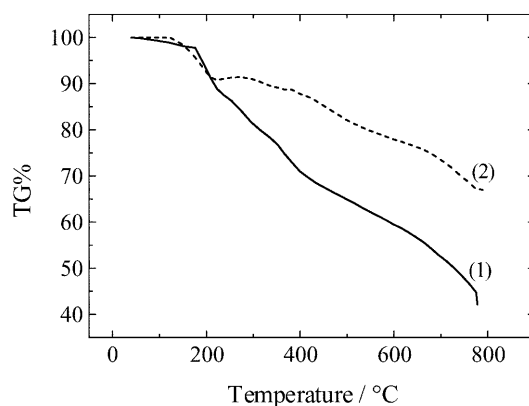


**Fig. 13** Thermogravimetric curves of (1) PPy film and (2) PPy film containing Ge microparticles; temperature sweep rate  $10 \text{ }^\circ\text{C min}^{-1}$

about 310 °C. Beyond this temperature range the mass continuously decreased to reach a weight loss about 33% at 750 °C. Apparently the thermal stability of the PPy films is increased if Ge microparticles are inserted.

#### Microscopy of a PPy film containing Ge microparticles

In order to confirm the presence of Ge particles in the matrix of the PPy film, a SEM examination coupled with an EDX analysis was performed. As observed in Fig. 14, the texture of the PPy film is granular and can be compared with the much coarser “cauliflower structure” which is commonly reported in the literature [30, 31]. The germanium microparticles can be seen as small bright spots of an average diameter less than 2 μm. A large amount of deposited Ge microparticles and their uniform distribution are seen.

EDX analysis of the PPy film containing Ge microparticles (Fig. 15), conducted with a very small electron

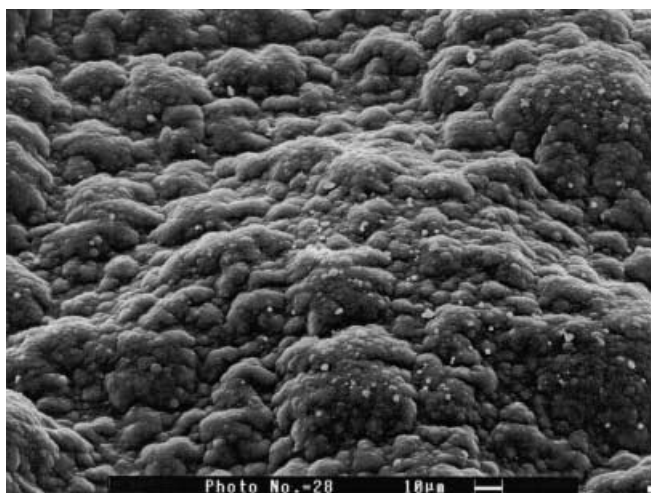


**Fig. 14** SEM picture of a PPy film containing Ge microparticles electrodeposited on a passivated titanium electrode; the Ge microparticles can be seen as bright spots of average diameter less than 2 μm

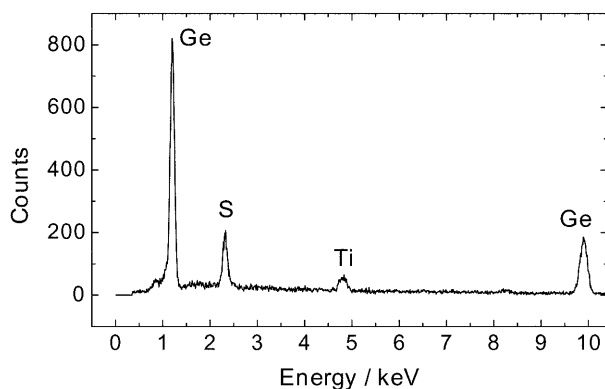


**Fig. 15** EDX analysis of the PPy/Ge surface coupled with the SEM analysis presented in Fig. 14

beam, confirms again the presence of germanium in the PPy film. The EDX analysis showed the presence of germanium, titanium and sulfur. These two latter elements were due to the substrate and the  $\text{SO}_4^{2-}$  anions (dissolution of germanium in hot sulfuric acid [12]).

#### Conclusion

From cyclic voltammetric, chronoamperometric and chronopotentiometric studies it follows that the passivated titanium electrode is a good substrate material for the preparation of PPy and Ge-modified PPy electrodes in acidic aqueous nitrate solutions. It was shown that the kinetics of oxidation of the monomer is controlled by its diffusion in solution. Also, it was found that growth of the PPy film did not passivate the titanium electrode.

Variation of the electrode surface area, caused by deposition of the PPy films, has been estimated from measurements of the double layer capacitance in order to determine the true current density.

Voltammetry showed that the polymer-modified electrode exerts a marked electrocatalytic effect on the reduction of both oxygen and protons. The reduction of protons and oxygen at the Ti/PPy/Ge electrodes depends on how the Ge particles are distributed in the polymer. For a long time for germanium deposition, most particles are located near the surface of the PPy film. Such a Ge insertion leads to a high reduction rate of oxygen and protons, because a large number of germanium reaction sites is available for reduction. When Ge microparticles are deposited at a lower Ge concentration in solution, they are more evenly distributed over the whole film, leading to a low reduction rate of oxygen and protons.

The PPy films serve as an excellent conducting matrix for dispersion of the Ge microparticles. The three-dimensional conducting film allows us to change distribution of the electrodeposited catalyst particles, by varying the deposition rate.

Based upon thermogravimetric analysis, Ge microparticle insertion in the PPy film leads to substantial changes in its structure.

**Acknowledgements** The authors thank Dr. H. Takenouti from UPR 15 du CNRS (Paris) for helpful discussions, his critical remarks and help during revising the manuscript.

#### References

1. Vork FTA, Jansen LJJ, Barendrecht E (1986) *Electrochim Acta* 31:1569
2. Vork FTA, Jansen LJJ, Barendrecht E (1987) *Electrochim Acta* 32:1187
3. McGee A, Cassidy JF, Quigley P, Vos JG (1992) *J Appl Electrochem* 22:678
4. Vork FTA, Barendrecht E (1990) *Electrochim Acta* 35:135
5. Lyons MEG (1994) *Analyst* 119:
6. Emr SA, Yacynych AM (1995) *Electroanalysis* 7:10
7. Josowicz M (1995) *Analyst* 120:
8. De la Fuente C, Acuna JA, Vasquez MD, Tascon ML, Gomez MI, Sanchez Batanero P (1997) *Talanta* 44:685



9. Tourillon G, Garnier F (1982) *J Electroanal Chem Interfacial Electrochem* 135:173
10. Prejza J, Lundström I, Skotheim T (1982) *J Electrochem Soc* 129:1685
11. Schirmeisen M, Beck F (1989) *J Appl Electrochem* 19:401
12. Kirk-Othmer (1981) *Encyclopedia of chemical technology*, vol 1. Wiley, New York, p 791
13. De Gregori I, Carrier M, Deronzier A, Moutet JC, Bedioui F, Devynck J (1992) *J Chem Soc Faraday Trans* 88:1567
14. Makhloufi L, Ymmel S, Khelifa N, Mezghiche H (1993) *Journ Electrochim Grenoble*, 7–10 juin, CA 6.1
15. Galal A (1998) *J Solid State Electrochem* 2:7
16. Cheung KM, Bloor D, Stevens GC (1988) *Polymer* 29:1709
17. Makhloufi L, Saidani B, Cachet C, Wiart R (1998) *Electrochim Acta* 43: 3159
18. Landolt D (1993) *Traité des matériaux, corrosion et chimie de surfaces des métaux*. Presses Polytechniques et Universitaires Romandes, Switzerland
19. Karakisla M, Saçak M, Erdem E, Akbulut U (1997) *J Appl Electrochem* 27:309
20. Tedjar F, Ymmel S, Janda M, Duchek P, Holy P, Stibor I (1989) *Collect Czech Chem Commun* 54:1299
21. Delahay P (1954) *New instrumental methods in electrochemistry*. Interscience, New York
22. Scharifker BR, Garcia-Pastoriza E, Marino W (1991) *J Electroanal Chem* 300:85
23. Anson FC, Oshaka T, Saveant JM (1983) *J Am Chem Soc* 104:4811
24. Miller LL, Zinger B, Zhou Q-Z (1987) *J Am Chem Soc* 109:2267
25. Hills G, Montenegro I, Scharifker B (1980) *J Appl Electrochem* 10:807
26. Palmisano F, Desimoni E, Sabbatini L, Torsi G (1979) *J Appl Electrochem* 9:517
27. Roberts JL, Sawyer DT (1987) *J Am Chem Soc* 109:8081
28. Holdcroft S, Funt BL (1988) *J Electroanal Chem* 240:89
29. Wang J, Chen S-P, Lin MS (1989) *J Electroanal Chem* 273:231
30. Qian R, Qiu J (1987) *Polym J* 19:157
31. Beck F, Oberst M (1987) *Macromol Chem* 8:97